Food Research 6 (5) : 56 - 67 (October 2022)
Journal homepage: https://www.myfoodresearch.com

FOOD RESEARCH

FULL PAPER

Effect of viscosity on iron encapsulation using alginate as a carrying agent in a controlled spray drying process

Permanadewi, I., *Kumoro, A.C., Wardhani, D.H. and Aryanti, N.

Department of Chemical Engineering, Faculty of Engineering, Diponegoro University, Indonesia

Article history:
Received: 10 August 2021
Received in revised form: 24 September 2021
Accepted: 19 January 2022
Available Online: 9 September 2022

Keywords:
Viscosity,
Encapsulated,
Iron,
Alginate,
Spray drying

DOI:
https://doi.org/10.26656/fr.2017.6(5).613

Abstract

The encapsulation method is a method that protects Fe from oxidation, increases bioavailability and reduces the unwanted taste, aroma, and distinctive colour of Fe. Alginate is used as an encapsulant because it can be regulated in viscosity. The drying process by spray drying is chosen to obtain the final product that has the appropriate quality standards. The purpose of this study was to determine the effect of alginate 50 mPas, 100 mPas, 150 mPas, 200 mPas, 250 mPas and 300 mPas viscosity on the characteristics of powder encapsulation. The results showed that the higher the viscosity, the darker the colour of the powder produced. Powder particle size increases with increasing viscosity; and the higher the viscosity, the higher the moisture content. The solubility of the alginate-Fe encapsulated powder was lower with increasing viscosity. The particle morphology shows a lot of indentation and unevenness, and the pore size is bigger at a viscosity of 150 mPas to 300 mPas. The alginate-Fe encapsulated powder of all viscosity variables showed the same functional groups but in different intensities. At the testing of Fe^{2+} levels, it turned out that Fe^{3+} had higher levels than Fe^{2+}. The process of releasing Fe^{2+} at pH 1.2 was slower than pH 6.8. From the research results, alginate-Fe encapsulation powder with a viscosity of 100 mPas produced the highest performance in protecting Fe, thus, a good viscosity of the feed solution was recommended in the spray drying process.

1. Introduction

One of the most widespread health problems in the world is anaemia. World Health Organization (WHO) (2021) estimates that 42% of children less than 5 years of age and 40% of pregnant women worldwide are anaemic. Anaemia can interfere with child development, immune mechanisms and brain development (Allali *et al.,* 2017). One way to prevent anaemia is by consumption of iron-rich foods.

Many parameters need to be taken into account in the manufacture of Fe fortified foods, such as iron bioavailability, taste, aroma, colour and ability to protect Fe from oxidation. The encapsulation method is a method that can protect Fe from undesirable conditions because encapsulation is a process, in which small particles in the core material are covered by a coating wall to form a capsule. This encapsulation method was developed to protect bioactive components from adverse environments and to control the release of the target compound (Lim *et al*., 2017). In the encapsulation process, the selection of the encapsulant material is an important factor so that the targeted active ingredient can be maximally protected. One of the potential materials, that can be utilized as iron due to its adjustable viscosity and remarkable solubility encapsulant is sodium alginate (Ching *et al.,* 2017). Thus far, sodium alginate is widely used as an encapsulant under alkaline conditions (Hariyadi and Nazrul, 2020). Several previous researchers have used sodium alginate as an encapsulation material because apart from food-grade, sodium alginate is also biocompatible. Like Martin *et al.* (2017) who used sodium alginate to encapsulate fish oil, there is Simo *et al.* (2017) encapsulated cells using sodium alginate. Atencio *et al.* (2020) used sodium alginate to encapsulate ginger oil and Volic *et al.* (2018) used sodium alginate to encapsulate essential oils. From some of these previous researchers, we can see that sodium alginate has been widely used as an encapsulation material that can protect the active substance from certain conditions.

Usually, the encapsulation of an important compound uses a controlled spray drying process

*Corresponding author.
Email: *andrewkomoro@che.undip.ac.id*

eISSN: 2550-2166
Published by Rynnye Lyan Resources

because this process is very suitable for the production of dry solids in the form of powders, granules from liquid raw materials that have acceptable quality standards in terms of particle size distribution, moisture content and particle shape (Assadpour *et al.,* 2019). The quality of the final product and the efficiency of the spray drying process depends on several parameters, including droplet size distribution, the airflow pattern in the air chamber column, inlet temperature, feed flow rate, and drying air flow rate (Moser *et al*., 2019). In the process of droplet size distribution, one of the influential factors is the viscosity of the feed solution. The greater the viscosity of the feed solution, the larger the resulting droplet size, in contrast, the smaller the viscosity of the feed solution, the smaller the droplet size (Arpagaus *et al*., 2018). This droplet size determination is an important step in the spray drying process to produce the desired powder size and particle shape (Tupuna *et al*., 2018). This study sought to obtain data that will help to address the effect of the viscosity of the encapsulant material, namely alginate, on the characteristics of the powder from the encapsulation process.

2. Materials and methods

2.1 Materials

The material used in this study was alginate (Food Grade) with a glass transition temperature value of 95.3° C, purity of 74%, the protein content of 32% and carbohydrate content of 21% (Buana Chem, PT. Eternal Buana Chemical Industries). Iron (II) Sulfate Heptahydrate has a water solubility of 48.6 g/100 mL at 50°C (Merck kGaA, Germany). Sodium acetate, 1,10-Phenanthroline, HCl and Phosphate buffer (Merck kGaA, Germany).

2.2 Preparation of Alginate-Fe solution

In this study, the viscosity used was in the range of 50-300 mPas. This is in accordance with the Eyella SD-1000 handbook where the maximum recommended viscosity is 300 mPas and the minimum viscosity is 50 mPas. Because according to Permanadewi *et al*. (2021), alginate viscosity below 50 mPas has a very low alginate concentration so that the yield produced by spray drying will be low as well. Based on Permanadewi's research (2021), an alginate-Fe solution with a viscosity of 50 mPas was prepared by mixing 8 g alginate and 4 g Fe in 2 L of water which was then stirred using a magnetic stirrer for 15 mins at a speed of 600 rpm at 30°C controlled using a water bath. For the preparation of alginate-Fe solution with a viscosity of 100 mPas, 150 mPas, 200 mPas, 250 mPas and 300 mPas solid masses of alginate (0.8%:0.4%, 1%:0.5%, 1.6%:0.8%, 2%:1% and 3.7%:1.85%) were performed in similar steps.

2.3 Alginate-Fe encapsulation using spray drying

The spray drying experiment in this research was performed using the EYELA Spray Dryer SD-1000 (Japan). This spraying system used a two-liquid nozzle consisting of an internal tip with a diameter of 0.71 mm. The operating conditions used were based on the Eyela SD-1000 Handbook where the inlet temperature, outlet temperature, atomization rate and dry air flow rate were set to 150°C, 85°C, 22.10 kPa and 0.95 m^3/min respectively for all experiments. The alginate-Fe solution that was sprayed had a viscosity of 50 mPas, 100 mPas, 150 mPas, 200 mPas, 250 mPas and 300 mPas.

2.4 Fourier-transform Infrared Spectroscopy (FTIR)

The functional group analysis of the alginate-Fe encapsulation powder was identified using Fourier transform infrared spectroscopy (FTIR) (Perkin Elmer Frontier TM, Perkin Elmer, Waltham, MA, USA). Infrared absorption spectra were recorded on an FTS-175 spectrometer with a spectral resolution and a wave-number accuracy of 4 cm^{-1} and 0.01 cm respectively. Working pressure of 70 cNm was used. Before the spectra of the samples were recorded, the sample compartment was flushed with N_2 gas to prevent disturbance by water and CO_2 (Lohumi *et al*., 2017).

2.5 Water content

The alginate-Fe encapsulation powders were analysed for their moisture content using the Association of Official Analytical Chemist method at a temperature of 135°C until constant weight (AOAC, 2018).

2.6 Colour

The colour analysis of alginate-Fe powder was observed using the CIELAB colour space method using a Chroma Meter (CR-300, Minolta, Japan) which results in the values a*, b* and L*. The a* value describes a mixed chromatic colour of red and green with +a* (positive) value from 0 to +80 for red and -a* (negative) value from 0 to -80 for green. The b* value describes the mixed chromatic colour of blue and yellow with +b * (positive) value from 0 to +70 for yellow and -b* (negative) value from 0 to -70. An L* value describes the brightness of the colour, 0 for black and 100 for white. The colour difference (E) of alginate-Fe powder is calculated using the formula $E = (L^*_0 - L^*)^2 + (a^*_0 - a^*)^2 + (b^*_0 - b^*)^2$, where the value of L^*_0, a^*_0 and b^*_0 are the colours of the original alginate powder without the addition of Fe (Hosseini *et al*., 2019).

2.7 Scanning Electron Microscope-Energy Dispersive X-Ray (SEM-EDX)

The particle morphology of the alginate-Fe

encapsulated powder was observed using scanning electron microscopy (JSM-6510 LV JEOL, Japan) at 15 kV, which was equipped with a dispersive X-ray point scanning energy (EDX) (Chuyen *et al*., 2019).

2.8 Transmission electron microscopy (*TEM*)

The particle morphology of the alginate-Fe encapsulation powder was examined in more depth using Transmission Electron Microscopy (TEM JEOL JEM 2100, Japan) at a magnification of 1 nm to 500 nm (Marwa *et al*., 2018).

2.9 Loading capacity

The iron content of alginate-Fe encapsulation powder was analyzed using the method of Veerabhadraswamy *et al*. (2018), with minor modifications, using a spectrophotometer (UV-vis 752 N). Alginate-Fe encapsulation powder (0.1 g) was dissolved in 20 mL of distilled water then added 8 mL of Na-acetate solution and 10 mL of 1,10-phenanthroline solution were then diluted to 50 mL. The solution mixture was allowed to stand for 10 mins for colour development. After that, the absorbance of the mixture was read with a UV-Vis spectrophotometer at a wavelength of 508 nm. Loading Capacity calculation was calculated using the formula:

$$\text{Loading Capacity (\%)} = \frac{\text{iron mass (mg)}}{\text{total solid mass (mg)}} \text{x } 100\% \quad (1)$$

2.10 Particle Size Analysis (PSA)

Particle size distribution was analysed using a particle size analyser (Laser Particle Sizer, LLPA-C10) at 25±1.0°C with a duration of 50 seconds and a measurement range of 0.01-2000 nm (Hariadi *et al*., 2020).

2.11 Release of Fe

The iron release profile was quantified in HCl solution pH 1.2 and phosphate buffer (0.1 M) pH 6.8. The alginate-Fe encapsulation powder of as much as 0.05 g was added to 20 mL of pH 1.2 or 6.8 solutions. The solution was put into the incubator shaker for 6 hrs with samples were taken every 30 mins. The sample was filtered with filter paper to take the filtrate (Whatnam 1001,090, Sigma Aldrich, diameter 90 mm). For the Fe^{2+} test, the filtrate was added with 8 mL of Na-acetate solution and 10 mL of 1,10-phenanthroline solution, which were then diluted to 50 mL. The mixture sits for 10 mins for colour development. The absorbance of the solution was measured with a UV-Vis spectrophotometer at a wavelength of 508 nm (Hoang *et al*., 2018).

Calculation of release kinetics in this study was calculated using the Korsmeyer-Peppas model. Korsmeyer-Peppas is a simple model known as the "Power-law" that describes drug release from polymer systems. The Korsmeyer-Peppas model describes several simultaneous release mechanisms such as diffusion of water into the matrix, swelling of the matrix and dissolution of the matrix (Permanadewi *et al*., 2019).

$$\frac{Ct}{C\infty} = kt^n \quad (2)$$

Where Ct/C∞ = fraction of drug release at time, k = rate constant and n = release exponent

2.12 Solubility

This solubility analysis is related to Fe release analysis. The final sample solution was analysed in the analysis of Fe release, both the pH 1.2 and pH 6.8 solutions were taken from the incubator shaker. After the sample was deposited, then the sludge was dried using an oven. Wet and dry sediment weights were weighed to determine solubility with the following formula (Neves *et al*., 2019).

$$\text{Solubility (\%)} = \frac{\text{dry sediment mass}}{\text{wet sediment mass}} \text{x} 100\% \quad (3)$$

2.13 Statistical Analysis

Six different experimental groups were conducted, and the entire study was replicated three times. The differences identified in the results of the analysis were calculated using the statistical calculation of the p-value. The data obtained by alginate-Fe encapsulation powder with differences in viscosity to moisture content, loading capacity, Fe release and solubility were evaluated by one -way analysis (ANOVA) from the variance technique with a probability level <0.05.

3. Results and discussion

3.1 Moisture content

Moisture content is one of the important food safety parameters. Water content can affect the taste, texture, weight, appearance and shelf life of food ingredients. The microbial growth rate in the food products increased with the higher moisture content due to higher water activity (Jung *et al*., 2018). Figure 1 shows the values of the water content of each alginate-Fe concentration where the moisture content of alginate-Fe powder range between 4-6%. At a viscosity of 50 mPas, the water content value is 4.21%, the viscosity of 100 mPas is 4.87%, the viscosity of 150 mPas is 5.14%, the viscosity of 200 mPas is 5.98%, the viscosity of 250 mPas is 6.32% and 300 mPas is 6.85%. Where according to the Food and Agriculture Organization (FAO, 2018) the maximum value of water content in powdered food is 5%. So that the Fe-alginate powder that meets FAO

standards in this study is a powder with a viscosity of 50 and 100 mPas. As shown in Figure 1, the water content of the Fe-alginate powder at a viscosity of 50 mPas is lower than that of the Fe-alginate powder at a viscosity of 250 mPas and the results of statistical calculations show a significant difference between the two viscosities (p<0.05). It is clear that the higher the feed solution viscosity, the higher the value of the moisture content obtained. This fact occurred because the high concentration of alginate makes the water is difficult to leave the matrix during the drying process. Alginate is a polymer with an excellent ability to hold water therefore the higher the alginate concentration, the stronger its ability to hold water (Singha *et al.,* 2018).

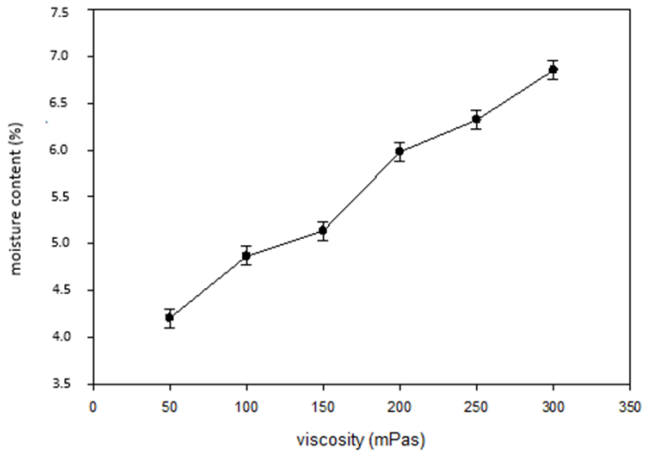

Figure 1. Moisture content of the alginate-Fe encapsulation powder at a viscosity of 50 mPas, 100 mPas, 150 mPas, 200 mPas, 250 mPas and 300 mPas

The water content is one of the most crucial quality aspects for product storage and stability (Khwanpruk *et al*., 2018) because water is one of the substances needed by microorganisms in their growth (Zambrano *et al*., 2019). The higher the water content, the higher the chance that microbes can grow. Although the moisture content after spray drying is an important consideration, the relative humidity of the storage environment also plays a role in determining long-term product stability (Patriani *et al*., 2020). In powders that have a high moisture content, the possibility of clumping during the storage period is greater than those with low water content, because the powders absorb moisture from the environment to achieve equilibrium conditions. In addition, the difference in humidity between the environment and the powder will cause a difference in the partial pressure of water vapour. This difference in partial pressure of water vapour will drive a transfer of water vapour from an area of high pressure to an area of low pressure. Because the partial pressure or humidity of the ambient air-water vapour is greater than the partial pressure of powdered water vapour in the package, water vapour will move into the powder (Jung *et al*., 2018). A powder that has a high water content will store more moisture and when its surface is moved by water, a bridge forms between the particles and the particles combine to cause clumping (Cheng *et al*., 2017).

3.2. Colour

The appearance of a product is one of the most important sensory qualities in fresh food products, processed products and marketing (Spence, 2019). The appearance of food was primarily determined by the colour of the food, where the colour is the first impression of the product by consumers. Colour is also an indicator of overheating and can be used to predict quality due to heat exposure, such as browning (Spence, 2018). Apart from the heat, the viscosity of the solution is also an indicator of colour differences. This viscosity is related to the concentration of solids dissolved in a solution. The higher the viscosity, the greater the number of dissolved solids thus far the resulting cloudy colour will also be cloudier (Phan *et al*., 2021). The colour properties of food powders were evaluated with HunterLab L*, a*, b* or CIE, and Hue. HunterLab L*, a*, b* and colour scale modified CIE system or called CIELAB are systems commonly used in the food industry (Schelkopf *et al*., 2021). Figure 2 suggests that the values of L and decrease with increasing viscosity of the alginate-Fe solution.

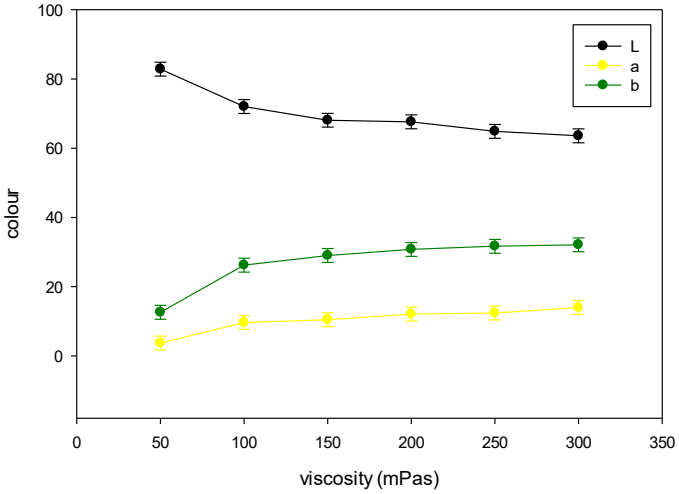

Figure 2. Lightness of alginate-Fe encapsulation powder at a viscosity of 50 mPas, 100 mPas, 150 mPas, 200 mPas, 250 mPas and 300 mPas.

The L and a-values of alginate-Fe powder at a viscosity of 100 mPas were 72.05 and 12.38, respectively. Their values were higher than the L and a-values of alginate-Fe powder at a viscosity of 300 mPas, which were only 63.59 and 3.71. The higher the viscosity of the alginate-Fe solution, the cloudier and the green colour of the alginate-Fe powder produced. In contrast to the value of b, which indicated that the higher the viscosity of the alginate-Fe solution, the higher the b value. As with the viscosity of 50 mPas, the value of b is 12.58, and the value of b increases to 30.76 at the

viscosity of 200 mPas, the increase in the value of b shows a significant difference in statistical calculations (p<0.05). The higher the viscosity of the alginate-Fe solution, the more yellow the colour of the alginate-Fe powder produced. This happens because the alginate powder itself has a yellowish-brown colour. In contrast, the Fe powder has a greenish-blue colour composition, therefore when it was put together in a solution, the resulting colour was yellowish-brown. Changes in the values of L, a and b in the alginate-Fe encapsulation powder prove that the total solid affects the colour of the spray drying powder.

The colour of the alginate-Fe powder was then compared to the difference in colour with the alginate powder that was not accompanied by the addition of Fe at the variation of the viscosity of the 50 mPas and 250 mPas solutions as in Figure 3. Figure 3 indicates the difference in the colours of L and a between alginate-Fe powder and alginate powder without addition Fe is negative. At the same time, the difference in colour b between alginate-Fe powder and alginate powder without the addition of Fe was positive. This shows that the colour of the alginate-Fe powder produced tends to be darker which is indicated by the low L and a-values compared to the original colour of the alginate without Fe which has a value of L_0* = 89.72, a_0* = 19.76, b_0* = 10.46 where statistically this colour difference showed a significant difference (p<0.05). The higher the viscosity of the alginate-Fe solution, the darker the colour of the powder produced. This is due to the non-enzymatic browning reaction during heating, the Maillard reaction. This Maillard reaction occurs because sodium alginate powder is known to contain 0.65% protein and 0.77% carbohydrates so that during heating a reaction occurs between reducing sugars and amines free of amino acids or proteins which then form a brown compound called melanoidin (Zhou *et al*., 2018).

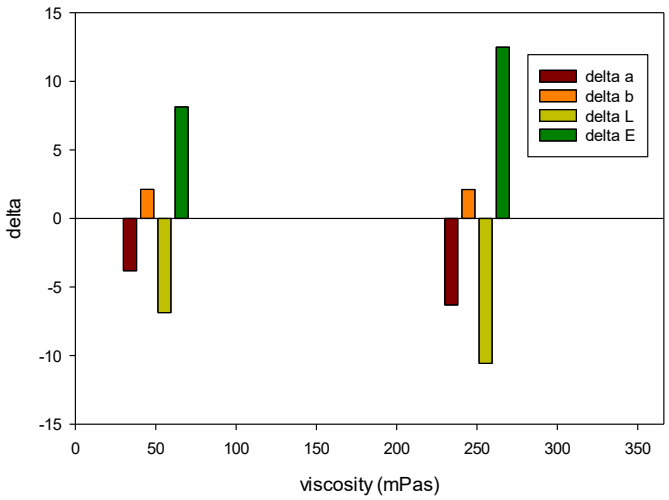

Figure 3. Analysis of the colour of the alginate-Fe encapsulation powder with a viscosity variation of 50 mPas and 250 mPas

3.3 Scanning Electron Microscope-Energy Dispersive X-Ray (SEM-EDX)

Morphological characterization of this alginate powder was analyzed using SEM (Scanning Electron Microscope) and EDX (Energy Dispersive X-ray Spectroscopy) methods with 5000x magnification. Figure 4 indicates that with the different viscosity of the solution, the shape and size of the particles obtained were also different. At low viscosities, the resulting droplets tend to be smaller than those at high viscosities. These droplets affected particle morphology. The bigger the droplets, the more rounded the resulting particle morphology but the surface was wrinkled, not smooth, with many indentations and holes like hollows. Such particle shape was caused by shrinkage during the final drying or cooling process of the particles containing relatively large air vacuoles (Guimaraes *et al*., 2020).

The vacuole was formed when water in the emulsion system evaporates due to the high temperature during the spray-drying process, and the water vapour was then trapped in a group of coated Fe particles. The air inside the microcapsule particles pressed the particle walls to get out. The higher the viscosity, the bigger the vacuole formed because the greater the air pressure in the microcapsule particles that presses the particle walls caused shrinkage during cooling. This shrinkage occurred after the spray drying process caused by the coating material, which was unable to maintain a spherical shape due to air pressure from inside the particles (Zujeva *et al*., 2017). In the EDX analysis not shown, the symbol elements that appear in all of the Fe-alginate powder samples are oxygen (O), carbon (C), nitrogen (N), sodium (Na), sulfur (S) and iron (Fe) where all the symbol elements are shows that the spray drying process does not change the elements present in the sodium alginate and Fe.

3.4 Particle size analysis

The particle size is one of the quality parameters in the drug release process. The size of the particles greatly affects the drug release performance. If the particle size is too large, the rate of drug degradation will be prolonged, but if the particle size is too small, the drug carrier matrix will enter the cell and settle in the cell, interfering with the cell cycle. The particle size of the matrix used as a drug carrier is 10-400 nm. The smaller the nanomaterial particle size, the lower its efficiency (Bastan *et al*., 2017). The particle size of the alginate-Fe encapsulation powder can be seen in Figure 5 where the particle size at a viscosity of 50 mPas to 300 mPas is in the range 9-17 nm.

At a viscosity of 50 to 150 mPas, the larger the

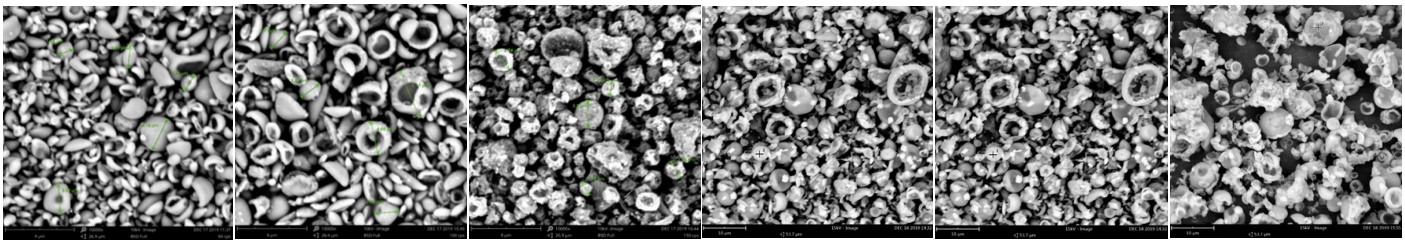

Figure 4. SEM characterization of alginate-Fe encapsulation powder at 5000× magnification formed at various viscosities of 50 mPas (a), 100 mPas (b), 150 mPas (c), 200 mPas (d), 250 mPas (e) and 300 mPas (f)

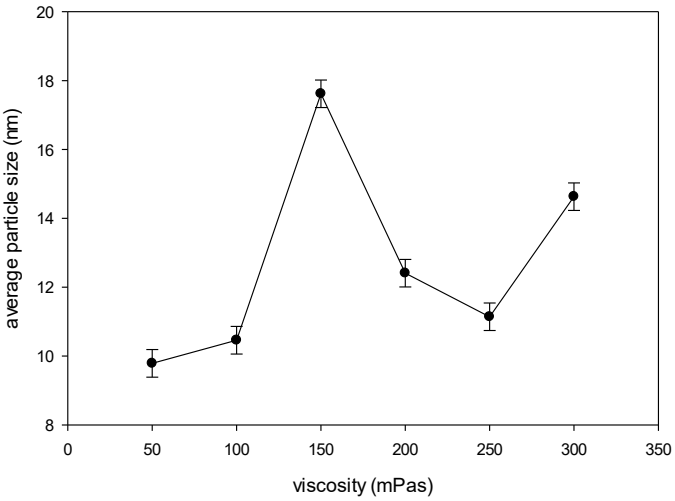

Figure 5. The average particle size of alginate-Fe powder at a viscosity of 50, 100, 150, 200, 250 and 300 mPas

particle size, but at a viscosity of 200 to 300 mPas there was a decrease in the particle size therefore it showed a significant difference between the two (p<0.05). This non-uniformity of particle size is influenced by the rate of evaporation, where the droplets that are not dried uniformly as a result of changes in heat energy in the dryer usually produce particles of different sizes (Zotarelli *et al*., 2017). In addition to the rate of evaporation and concentration, the distribution of particle size is also influenced by the intake temperature of the drying air, the feed flow rate and atomization (Tontul and Topuz, 2017).

3.5 Transmission electron microscopy

Transmission electron microscopy (TEM) analysis in this study was employed to analyze the microstructure of alginate-Fe encapsulation powder. Figures 6a to 6f illustrated TEM results of the Fe-alginate encapsulated powder. Figures 6a and 6b show the microstructure with small and dense pores, while in Figures 6c to 6f the pores were bigger. These results suggested that the alginate-Fe encapsulation powder at a viscosity of 150 mPas to 300 mPas had a brittle microstructure when compared to the microstructure of alginate-Fe powder at a viscosity of 50 mPas and 100 mPas. According to Desai (Laier *et al*., 2019), the presence of pores in the microstructure can be considered as the starting point for the breakdown of the alginate-Fe encapsulation powder. These pores usually occurred in processes that use high temperatures and pores with a large amount of coordination tend to appear during thermal processing. The higher the viscosity, the larger the pores in the microstructure of the alginate-Fe encapsulation powder. This fact corroborated with the SEM analysis that the higher the viscosity, the bigger and the more vacuoles formed in the alginate-Fe encapsulation powder.

3.6 Loading capacity

The loading capacity of alginate-Fe powder was significantly affected by the alginate concentration in the solution. With increasing concentration, the alginate viscosity and loading capacity will increase. This increase happens because, with increasing viscosity, the ability of alginate to absorb and then coat Fe also increases (Filho *et al*., 2019). Figure 7 shows an increase in loading capacity along with the rise in alginate viscosity. The increase in loading capacity of alginate-Fe powder is in the range of 82-89%. When the alginate-Fe solution was at a viscosity of 50 mPas, the amount of encapsulated Fe was only 82.3% different from the alginate-Fe solution at a viscosity of 300 mPas, the amount of encapsulated Fe reached 89.9% this showed a significant difference (p<0.05).

One of the benefits of the encapsulation method in this research was that it protected the active substance of

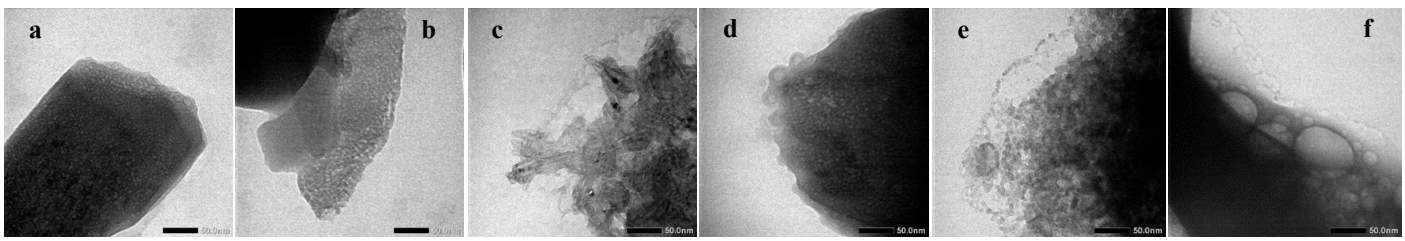

Figure 6. Characterization of TEM alginate-Fe encapsulation powder at a magnification of 50 nm with a viscosity variation of 50 mPas (a), 100 mPas (b), 150 mPas (c), 200 mPas (d), 250 mPas (e) and 300 mPas (f)

Fe to avoid the effects of oxidation. Oxidation is one of the undesirable factors in the manufacture of alginate-Fe encapsulation powder. Therefore, Fe^{2+} testing was carried out in this study. Figure 8 illustrates that the increase in Fe^{2+} levels only reached the alginate-Fe powder with a solution viscosity of 100 mPas, after which the Fe^{2+} levels decreased along with the increase in viscosity alginate-Fe solution that there was a significant difference between 100 mPas and 150 mPas solutions (p<0.05). This fact occurred because the higher the viscosity of the alginate-Fe solution, the more vacuoles were formed on the surface of the powder, the cause of which has been previously explained in the SEM analysis. Based on their observation, Tan *et al.* (2018) found that the shape of the particles with a lot number of vacuoles causes the active component (Fe) to be not located at the centre of the particles. However, it was located or bound to the matrix wall so that Fe was not entirely protected by alginate and caused oxidation of Fe.

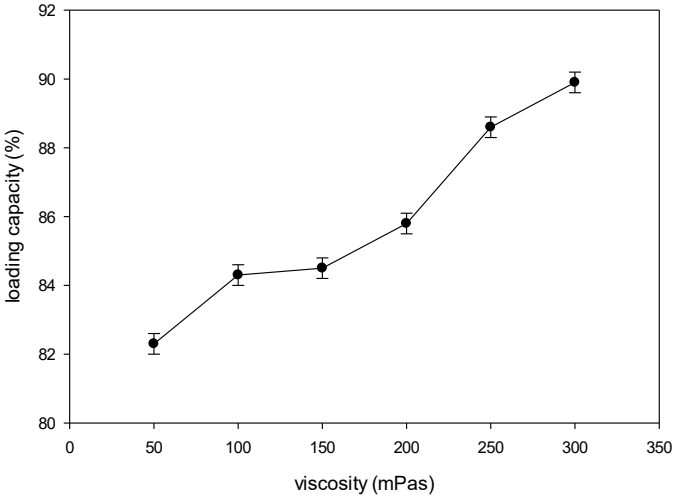

Figure 7. Loading capacity of alginate-Fe encapsulated powder at a viscosity of 50 mPas, 100 mPas, 150 mPas, 200 mPas, 250 mPas and 300 mPas

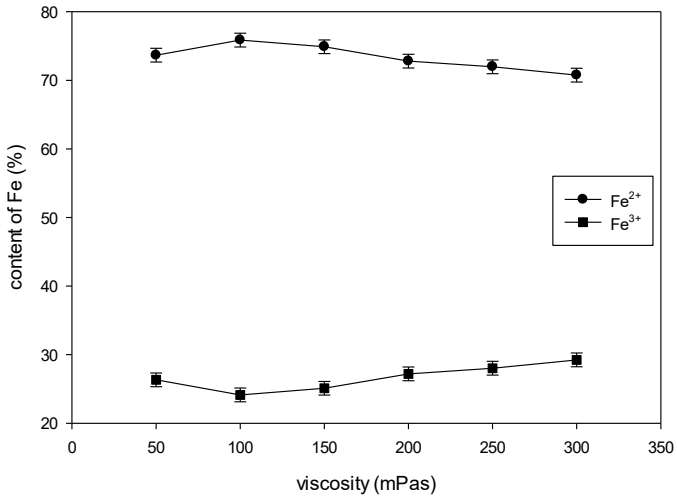

Figure 8. The content of Fe^{2+} and Fe^{3+} in the alginate-Fe encapsulation powder at a viscosity of 50 mPas, 100 mPas, 150 mPas, 200 mPas, 250 mPas, and 300 mPas

3.7 Fourier-transform infrared spectroscopy

Infrared spectrum analysis is an analysis to determine certain specific groups contained in complex compounds, either directly coordinated with the central ion or those that are not coordinated with the central ion. FTIR spectroscopic analysis in this study was based on the characteristics of the functional groups present in the six samples of alginate-Fe encapsulation powder. The FTIR spectrum data of each sample was obtained from the results of scanning the sample with the IR Prestige-21 Shimadzu tool in the IR region with a wavelength of 4000-400 cm^{-1}. The results of the FTIR spectrum of the alginate-Fe encapsulation powder can be seen in Figure 9. Figure 9 consists of a combination of 7 graphs, namely FTIR graphs with alginate-Fe viscosity of 50 mPas, 100 mPas, 150 mPas, 200 mPas,

Figure 9 at 3510.45 cm^{-1}, a wide absorption appeared, indicating a vibration of the O-H group in H_2O, which is in accordance with the theory around 3500 -3200 cm^{-1} (Chuangs *et al*., 2017). The sharp absorption in the area of 2413.5 cm^{-1} indicates that the C = O bond absorption of the carbonyl group. The bond was very strong in the area of 2500-2225 cm^{-1}. The sharp peak in the area of 1614.5 cm^{-1} indicated the presence of the C = C alkene group that appeared following the theory of 1680-1620 cm^{-1}. The sharp absorption at 1429 cm^{-1} indicated the presence of Na groups in the alginate isomer that appeared, according to the theory of 1614-1425 cm^{-1}. The sharp peak in the area of 1105.2 cm^{-1} also occurred due to the presence of the C-O carboxyl group, which in theory appears at 1200-1050 cm^{-1}. The aliphatic C-C aromatic compound appears at 883 cm^{-1} with a sharp peak, where according to the theory, the bond is strong in the area 1000-782.2 cm^{-1} The sharp peak in the area of 656.7 cm^{-1} indicated the absorption of Fe-OH compounds, which according to theory the bond, is strong in the area of 798-625 cm^{-1}. However, in the alginate powder that was not spray dried, the absorption of this Fe-OH compound did not appear. So from Figure 9, it can be concluded that spray drying does not affect the functional groups which show that the alginate does not degrade.

3.8 Solubility

The solubility analysis of alginate-Fe powder was closely related to the content of Fe in the alginate powder and whether or not the alginate-Fe encapsulated powder was dissolved in a solution. The effect of alginate concentration on the solubility percentage of alginate-Fe encapsulated powder in a solution of pH 1.2 and 6.8 can be seen in Figure 10. In Figure 10, it can be seen that the higher the alginate viscosity, the higher the solubility level of the alginate-Fe encapsulation powder. This is

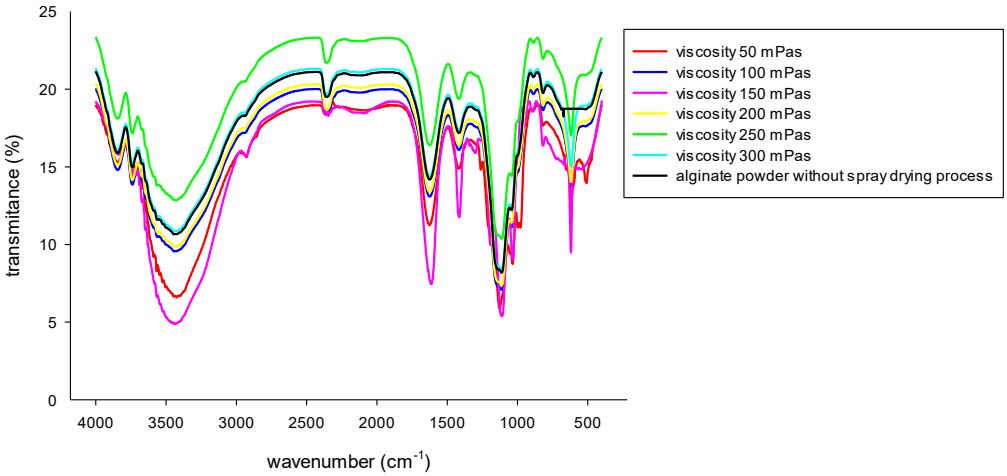

Figure 9. Comparison of FTIR spectrum for alginate-Fe encapsulated powder at a viscosity of 50 mPas, 100 mPas, 150 mPas, 200 mPas, 250 mPas, 300 mPas and alginate powder without spray drying process.

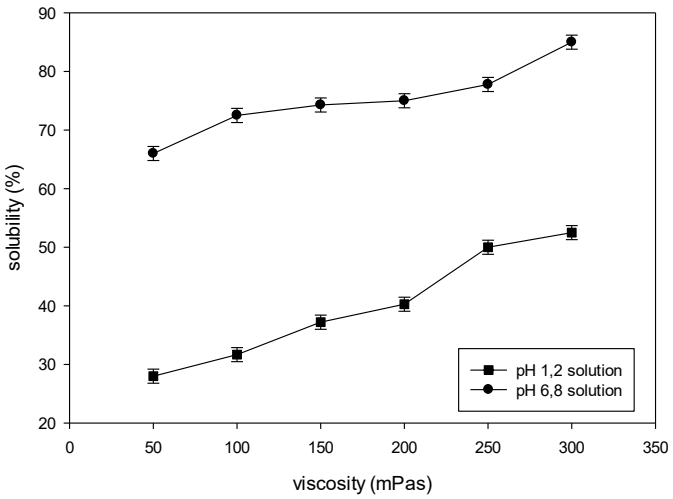

Figure 10. Solubility of alginate-Fe encapsulation powder at viscosity variations of 50, 100, 150, 200, 250 and 300 mPas in pH 1.2 and pH 6.8 solutions

related to the previous analysis, namely water content, where the higher the viscosity, the higher the water content contained. With the high water content, the higher the ability of the particles to absorb water on the surface so that the time for wetting because of the liquid is faster, where the ability to wet because this liquid can penetrate directly into the pores (Strobel *et al*., 2019). In addition, according to Lucas *et al*. (2020) The hydroxyl group in alginate will interact with water when the material is dissolved, the more hydroxyl groups, the higher the solubility level.

The solubility level of alginate-Fe powder in a solution of pH 6.8 was higher than that of alginate-Fe powder in a solution of pH 1.2. In pH 1.2 solution, the highest solubility level of alginate-Fe encapsulation powder was only 52.5%, namely at 50 mPas alginate viscosity which then decreased to 28% at 300 mPas viscosity. In contrast to the conditions of the pH 6.8 solution, the highest solubility level of alginate-Fe encapsulation powder reached 85%, namely at a viscosity of 50 mPas which then decreased to 66% at a viscosity of 300 mPas and this showed a significant difference between the two (p<0.05). According to Waterhouse *et al*. (2017), sodium alginate has a pK value of 3.38 for mannuronic acid monomer and pKa 3.65 for guluronic acid monomer so that sodium alginate will ionize in alkaline media and insoluble in acidic medium.

3.9 Release of Fe

Analysis of the release of Fe is one way to determine whether alginate is able to protect Fe from pH conditions in the digestive tract during the digestive process. Figure 11 shows the percentage of iron released from the microcapsules in HCl solution pH 1.2 and phosphate solution pH 6.8. These two pH solutions are often used in *in vitro* bioavailability studies because they are close to conditions such as those in the stomach and intestines (Singh *et al*., 2017). During the process of releasing Fe^{2+} in a solution of pH 1.2, which is a simulation of gastric fluid, the particles swell up which prompts Fe^{2+} to escape from the matrix. However, when this condition occurs, the particles are still in a solid-state and the swelling process occurs, the particles absorb water and provide little opportunity for further Fe^{2+} release. This equilibrium swelling is formed in about 120 mins. Then the observation of Fe release was continued using a pH 6.8 solution according to the simulation of intestinal fluid. In this condition, the swollen equilibrium is formed in about 200 mins, Fe^{2+} is released by diffuse mechanisms or particle erosion. After the swelling equilibrium, there is a steady increase in cumulative discharge reaching a plateau of about 80%.

From Figure 11, it can be seen that the process of releasing Fe^{2+} in a solution of pH 1.2 is not more than 50% for 3 hours. The highest Fe^{2+} release was in alginate powder with a viscosity of 300 mPas. While the lowest Fe^{2+} release was in alginate powder at a viscosity of 50 mPas. At pH 6.8, the Fe^{2+} release process shows a greater percentage than at pH 1.2. The highest Fe^{2+}

release was in alginate-Fe powder with a viscosity of 100 mPas which reached 80% and the lowest percentage of Fe^{2+} release was 60% in alginate-Fe powder with a viscosity of 300 mPas. The higher the viscosity, the more Fe^{2+} will be released from the powder. This is related to the previous analysis, namely solubility. When the powder passes through the gastric juices with an acidic pH, the alkaline character will be protonated and when the drug passes through the intestine with an alkaline pH, the acidic nature will be protonated. The base in the alkaline medium will remain in the molecule but if it is in the acidic medium, it will be protonated, and vice versa (Mishra *et al*., 2021).

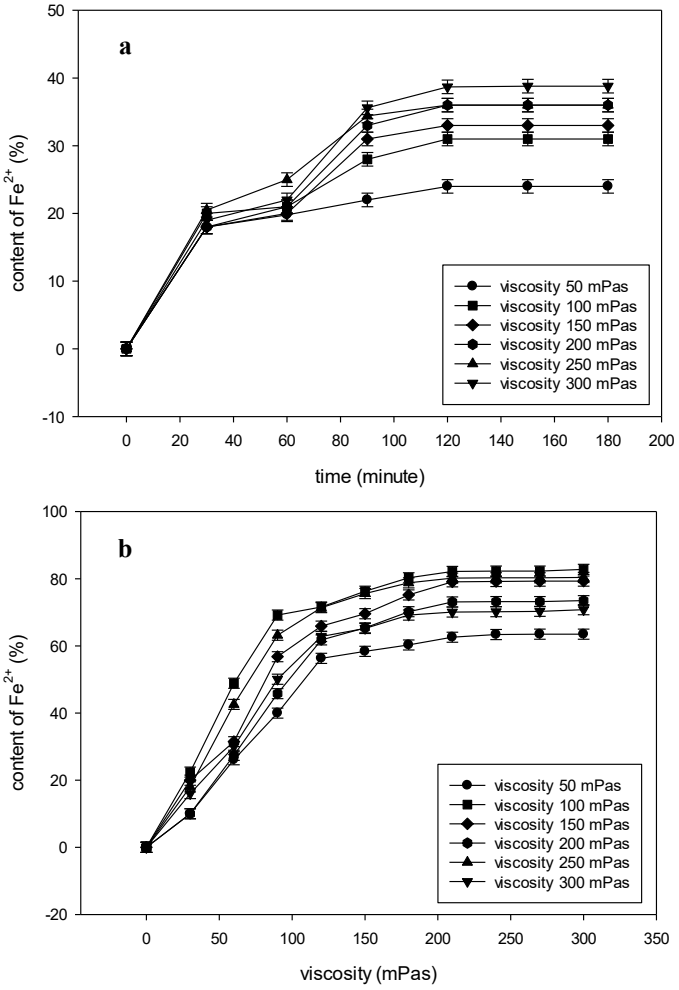

Figure 11. Release of Fe^{2+} from deep alginate-Fe encapsulation powder (a) pH 1.2 solution, (b) pH 6.8 solution

Table 1 shows the constants and coefficients of determination of the Korsmeyer-Peppas model. From Table 1, it can be seen that the highest R^2 value of this model at pH conditions of 1.2 and 6.8 is at a viscosity of 100 mPas, namely 0.985 and 0.983. The release exponent of Korsmeyer-Peppas (n) for conditions of pH 1.2 < 0.5 while at pH 6.8 > 0.5. The value of n indicates the mechanism by which the active compound is released from the matrix. In this case, the solvent diffusion is much larger than the polymer chain relaxation process. The kinetics of this phenomenon is characterized by diffusivity. Although the value of n at pH 1.2 is lower than 0.5, this value still indicates a diffusion-controlled drug release mechanism. If n is less than 0.5 in the case of the encapsulated spherical shape, then a Fickian diffusion release mechanism is implied (Permanadewi *et al*., 2021).

Table 1. The constants and coefficient of determinations (R^2) model Korsmeyer-Peppas

Data	Korsmeyer-Peppas		
	K	n	R^2
Gastric simulation fluid (pH 1.2)			
Viscosity 50 mPas	0.129	0.213	0.932
Viscosity 100 mPas	0.153	0.245	0.985
Viscosity 150 mPas	0.189	0.253	0.951
Viscosity 200 mPas	0.212	0.267	0.963
Viscosity 250 mPas	0.267	0.271	0.956
Viscosity 300 mPas	0.321	0.289	0.971
Intestinal simulation fluid (pH 6.8)			
Viscosity 50 mPas	0.565	0.429	0.967
Viscosity 100 mPas	0.692	0.431	0.983
Viscosity 150 mPas	0.703	0.452	0.965
Viscosity 200 mPas	0.741	0.469	0.931
Viscosity 250 mPas	0.813	0.478	0.945
Viscosity 300 mPas	0.825	0.488	0.973

4. Conclusion

Characterization of alginate-Fe encapsulation powder with variable viscosity of feed solution 50, 100, 150, 200, 250 and 300 mPas suggested that with increasing viscosity, the colour of the obtained powder was darker. Powder particle size increases with increasing viscosity and the higher the viscosity, the higher the moisture content where the powder according to the FAO moisture content standard is 50 mPas and 100 mPas. The solubility of the alginate-Fe encapsulated powder was lower with increasing viscosity. The particle morphology shows a lot of indentation and unevenness, and the pore size is bigger at a viscosity of 150 mPas to 300 mPas, while at a viscosity of 50 mPas and 100 mPas it shows a fine powder surface with smaller pores. The alginate-Fe encapsulated powder of all viscosity variables showed the same functional groups but in different intensities. The amount of encapsulated Fe appears to have a higher level with increasing viscosity. However, after further testing of Fe^{2+} levels, it turned out that Fe^{3+} had higher levels than Fe^{2+}. The process of releasing Fe^{2+} at pH 1.2 was slower than pH 6.8. In summary, these results indicated that the alginate-Fe encapsulation powder with a viscosity of 100 mPas showed the highest performance in protecting Fe. Therefore, a viscosity of 100 mPas is recommended as a suitable viscosity of the feed solution in the spray drying process.

Conflict of interest

The authors declare no conflict of interest.

Acknowledgements

This work was funded by the Directorate General of Research and Community Service, Ministry of Research Technology/National Agency for Research and Innovation, Republic of Indonesia, through Disertasi Doktor scheme-2020 (Grant number: 101-186/UN7.6.1/PP/2020).

References

Allali, S., Valentine, B., Anne, S.S., Martin, C. and Mariane, D.M. (2017). Anemia in Children: Prevalence Causes, Diagnostic Work-up and Long Term Consequences. *Expert Review of Hematology*, 10(11), 1023-1028. https://doi.org/10.1080/17474086.2017.1354696

Arpagaus, C., Andreas, C., David, R., Elham, A. and Seid, M.J. (2018). Nano Spray Drying for Encapsulation of Pharmaceuticals. *International Journal of Pharmaceutics*, 546(1-2), 194-214. https://doi.org/10.1016/j.ijpharm.2018.05.037

AOAC (Association of Official Agricultural Chemists). (2018). Determination of Moisture Content. AOAC 930.15. USA: AOAC.

Atencio, S., Alicia, M., Esther, S., Jose, M.G. and Carmen, G. (2020). Encapsulation of Ginger Oil in Alginate Based Shell Materials. *Food Bioscience*, 37, 100714. https://doi.org/10.1016/j.fbio.2020.100714

Bastan, F.E., Erdogan, G., Moskalewicz, T. and Ustel, F. (2017). Spray Drying of Hydroxyapatite Powders: The Effect of Spray Drying Parameters and Heat Treatment on the Particle Size and Morphology. *Journal of Alloys and Compounds,* 724, 586-596. https://doi.org/10.1016/j.jallcom.2017.07.116

Cheng, J.Y.K., Sam, L.H.C. and Irene, M.C.L. (2017). Effect of Moisture Content of Food Waste on Residue Separation, Larval Growth and Larval Survival in Black Soldier Fly Bioconversion. *Waste Management*, 67, 315-323. https://doi.org/10.1016/j.wasman.2017.05.046

Ching, S.H., Nidhi, B. and Bhesh, B. (2017). Alginate Gel Particles – A Review of Production Technique and Physical Properties. *Critical Reviews in Food Science and Nutrition*, 57(6), 1133-1152. https://doi.org/10.1080/10408398.2014.965773

Chuangs, J., Yu-Ya, H., Szu-Hsuan, L., Tzu-Fang, H., Wen-Ying, H., Shu-Ling, H. and Yung-Sheng, L. (2017). Effects of pH on the Shape of Alginate Particles and Its Release Behavior. *Hindawi International Journal of Polymer Science,* 2017, 3902704. https://doi.org/10.1155/2017/3902704

Chuyen, H.V., Paul, D.R., John, B.G., Sophie, E.P. and Minh, H.N. (2019). Encapsulation of Carotenoid-Rich Oil from Gac Peel: Optimisation of the Encapsulating Process using a Spray Drier and the Storage Stability of Encapsulated Powder. *Powder Technology,* 344, 373-379. https://doi.org/10.1016/j.powtec.2018.12.012

Food and Agriculture Organization (FAO). (2018). Standard for Milk Powders and Cream Powder, CXS 207-1999. Retrieved from FAO website: https://www.fao.org/fao-who-codexalimentarius/sh-proxy/en/?lnk=1&url=https%253A%252F%252Fworkspace.fao.org%252Fsites%252Fcodex%252FStandards%252FCXS%2B207-1999%252FCXS_207e.pdf

Filho, L.C.C., Maria, M.L., Margarida, M.M. and Vitor, D.A. (2019). Microencapsulation of B-Carotene by Spray Drying : Effect of Wall Material Concentration and Drying Inlet Temperature. *International Journal of Food Science,* 2019, 8914852. https://doi.org/10.1155/2019/8914852

Hariadi, H., Sunyoto, M., Nurhadi, B. and Karuniawan, A. (2020). Study of Drying Method Types on the Physicochemical Characteristics of Purple-Fleshed Sweet Potato Extract Powder. *Progress in Colour, Colorants and Coating,* 13, 41-51.

Hariyadi, D.M. and Nazrul, I. (2020). Current Status of Alginate in Drug Delivery. *Advances in Pharmacological and Pharmaceutical Science,* 2020, 8886095. https://doi.org/10.1155/2020/8886095

Hoang, D.L., Kurt, D.R., Ellen, L.K.D., Jie, F., Simon, A.M., Yingyue, Z., William, D.M., Hanu, R., Anil, P. and Robert, K.P. (2018). Encapsulation of OZ439 into Nanoparticles for Supersaturated Drug Release in Oral Malaria Theraphy. *ACS Infectious Diseases*, 4, 970-979. https://doi.org/10.1021/acsinfecdis.7b00278

Hosseini, H., Mohammad, G., Seid, M.J. and Alireza, S.M. (2019). Encapsulation of EPA and DHA Concentrate from *Kilka* Fish Oil by Milk Proteins and Evaluation of its Oxidative Stability. *Journal of Food Science and Technology,* 56(1), 59-70. https://doi.org/10.1007/s13197-018-3455-9

Jung, H., Youn, J.L. and Won, B.Y. (2018). Effect of Moisture Content on the Grinding Process and Powder Properties in Food : A Review. *Processes*, 6 (6), 69. https://doi.org/10.3390/pr6060069

Khwanpruk, K., Chanida, A., Patipan, W., Worakarn, K. and Suttiphat, C. (2018). Effect of Drying Air

Condition and Feed Composition on the Properties of Orange Juice Spray dried Powder. *MATEC Web of Conferences*, 192, 03013. https://doi.org/10.1051/matecconf/201819203013

Laier, C.H., Tommy, S.A., Mia, T.B., Pernille, B.S., Thomas, R., Anja, B. and Line, H.N. (2019). Evaluation of the Effect of Spray Drying Parameters for Producing Cubosome Powder Precursors. *European Journal of Pharmaceutics and Biopharmaceutics,* 135, 44-48. https://doi.org/10.1016/j.ejpb.2018.12.008

Lohumi, S., Ritu, J., Lalit, M.K., Hoonsoo, L., Moon, S.K., Hyunjeong, C., Changyeun, M., Young-Wook, S., Anisur, R. and Byoung-Kwan, C. (2017). Quantitative Analysis of Sudan Dye Adulteration in Paprika Powder using FTIR Spectroscopy. *Food Additives and Contaminants*, 34(5), 678-686. https://doi.org/10.1080/19440049.2017.1290828

Lucas, J., Mathis, R., Berta, N.E. and Fernando, R. (2020). A New Approach for the Microencapsulation of Curcumin by a Spray Drying Method, in Order to Value Food Products. *Powder Technology*, 362, 428-435. https://doi.org/10.1016/j.powtec.2019.11.095

Martin, E., Denis, P., Ramila, C.R. and Denis, R. (2017). Oil Encapsulation Techniques using Alginate as Encapsulating Agent: Applications and Drawbacks. *Journal of Microencapsulation*, 34(8), 754-777. https://doi.org/10.1080/02652048.2017.1403495

Marwa, M.E., Tamer, M.E. and Hala, M.F.E. (2018). The Encapsulation of Powdered Doum Extract in Liposomes and its Application in Yoghurt. *Acta Scientiarum Polonorum Technologia Alimentaria*, 17 (3), 235-245. https://doi.org/10.17306/J.AFS.0571

Mishra, A., Vipul, K.P., Bhavani, S.S. and Jose, S.M. (2021). Spray Drying as an Efficient Route for Synthesis of Silica Nanoparticles-Sodium Alginate Biohybrid Drug Carrier of Doxorubicin. *Colloids and Surfaces B: Biointerfaces,* 197, 111445. https://doi.org/10.1016/j.colsurfb.2020.111445

Neves, M.I.L., Sylvie, D.B., Italo, T.P., Stephane, D. and Jeremy, P. (2019). Encapsulation of Curcumin in Milk Powders by Spray Drying : Physcochemistry, Rehydration Properties, and Stability During Storage. *Powder Technology*, 345, 601-607. https://doi.org/10.1016/j.powtec.2019.01.049

Permanadewi, I., Kumoro, A.C., Wardhani, D.H. and Aryanti, N. (2019). Modelling of Controlled Drug Release in Gastrointestinal tract Simulation. IOP Conference Series: Journal of Physics: Conference Series, 1295, 012063. https://doi.org/10.1088/1742-6596/1295/1/012063

Permanadewi, I., Kumoro, A.C., Wardhani, D.H., Aryanti, N. (2021). Matemathical Approach for Estimation of Alginate-Iron Salt Solutions Viscosity at Various Solid Concentrations and Temperatures. *Current Research in Nutrition and Food Science*, 9 (1), 75-87. https://doi.org/10.12944/CRNFSJ.9.1.08

Phan, K., Truong, T., Wang, Y. and Bhandari, B. (2021). Effect of CO_2 Nanobubbles Incorporation on the Viscosity Reduction of Fruit Juice Concentrate and Vegetable Oil. *International Journal of Food Science and Technology,* 56(9), 4278-4286. https://doi.org/10.1111/ijfs.15240

Schelkopf, C.S., Emily, A.R., Joanna, K.S., Ann, M.H., Ifigenia, G., Keith, E.B. and Mahesh, N.N. (2021). Nix Pro Color Sensor Provides Comparable Color Measurements to HunterLab Colorimeter for Fresh Beef. *Journal of Food Science and Technology*, 58, 3661-3665. https://doi.org/10.1007/s13197-021-05077-6

Singh, A.P., Juveria, S., and Levente, L. (2017). Characterizing the pH-Dependent Release Kinetics of Food-Grade Spray Drying Encapsulated Iron Microcapsules for Food Fortification. *Food Bioprocess Technology*, 11(2), 435-446. https://doi.org/10.1007/s11947-017-2022-0

Singha, P., Kasiviswanathan, M. and Padmanaban, K. (2018). Influence of Processing Conditions of Apparent Viscosity and System Parameters during Extrusion of Distiller's Dried Grains based Snacks. *Food Science and Nutrition*, 6(1), 101-110. https://doi.org/10.1002/fsn3.534

Simo, G., Encarnacion, F.F., Josefina, V.C., Violeta, R. and Jose, M.R.N. (2017). Research Progress Incoating Techniques of Alginate Gel Polymer for Cell Encapsulation. *Carbohydrate Polymer*, 170, 1-14. https://doi.org/10.1016/j.carbpol.2017.04.013

Spence, C. (2019). On the Changing Colour of Food and Drink. *International Journal of Gastronomy and Food Science,* 17, 100161. https://doi.org/10.1016/j.ijgfs.2019.100161

Spence, C. (2018). Background Colour and Its Impact on Food Perception and Behaviour. *Food Quality and Preverence*, 68, 156-166. https://doi.org/10.1016/j.foodqual.2018.02.012

Strobel, S.A., Herbert, B.S., Nitin, N. and Tina, J. (2019). Control of Physicochemical and Cargo Release Properties of Cross-Linked Alginate Microcapsules formed by Spray Drying. *Journal of Drug Delivery Science and Technology,* 49, 440-447. https://doi.org/10.1016/j.jddst.2018.12.011

Tan, S., Tingting, J. and Amirali, E.T.L. (2018). Effect of Spray Drying Temperature on the Formation of Flower-Like Lactose for Griseofulvin Loading.

European Journal of Pharmaceutical Science, 111, 534-539. https://doi.org/10.1016/j.ejps.2017.10.040

Tontul, I. and Topuz, A. (2017). Spray-drying of Fruit and Vegetable Juices: Effect of Drying Conditions on the Product Yield and Physical Properties. *Trends in Food Science and Technology*, 63, 91–102. https://doi.org/10.1016/j.tifs.2017.03.009

Veerabhadraswamy, M., Devaraj, T.D. and Jayanna, B.K. (2018). Second Derivative Spectrophotometric Determination of Iron(II) and Ruthenium(III) Using 1, 10-phenanthroline. *Analytical Chemistry Letters*, 8 (6), 757–768. https://doi.org/10.1080/22297928.2018.1548944

Volic, M., Ivana, P.L., Verica, D., Zorica, K.J., Ilinka, P., Zora, S.D., Dorde, V., Miroslav, H. and Branko, B. (2018). Alginate/Soy Protein System for Essential Oil Encapsulation with Intestinal Delivery. *Carbohydrate Polymers,* 200, 15-24. https://doi.org/10.1016/j.carbpol.2018.07.033

Waterhouse, G.I.N., Dongxiao, S.W., Guowan, S., Haifeng, Z. and Mouming, Z. (2017). Spray-Drying of Antioxidant-Rich Blueberry Waste Extracts; Interplay Between Waste Pretreatments and Spray-Drying Process. *Food Bioprocess Technology*, 10, 1074-1092. https://doi.org/10.1007/s11947-017-1880-9

World Health Organization (WHO). (2021). Haemoglobin Concentrations for The Diagnosis of Anemia and Assessment of Severity, Vitamin and mineral Nutrition Information System. Geneva: WHO.

Zambrano, M.V., Baishali, D., Donald, G.M., Heather, L.M. and Marianne, F.T. (2019). Assessment of Moisture Content Measurement Methods of Dried Food Products in Small-Scale Operations in Developing Countries: Review. *Trends in Food Science and Technology*, 88, 484-496. https://doi.org/10.1016/j.tifs.2019.04.006

Zujeva, A.S., Zilgma, I. and Liga, B.C. (2017). Controlling the Morphology of Ceramic and Composite Powders Obtained via Spray Drying-A Review. *Ceramics International*, 43(15), 11543-11551. https://doi.org/10.1016/j.ceramint.2017.05.023

Zotarelli, M.F., Vanessa, M.S., Angelise, D., Miriam, D.H. and Joao, B.L. (2017). Production of Mango Powder by Spray Drying and Cast-tape Drying. *Powder Technology*, 305, 447-454. https://doi.org/10.1016/j.powtec.2016.10.027

